Electronic Supplementary Material (ESI) for CrystEngComm.

Supplementary Material for **"New insights into the role of additive anions in Mg^{2+} dehydration: implications for mineral carbonation"**

Dimitrios Toroz,[a] Fu Song,[a] Greg Chass,[a,b,c] and Devis Di Tommaso *[a]*

[a] School of Biological and Chemical Sciences, Queen Mary University of London, Mile End Road, London, E1 4NS, United Kingdom

[b] Department of Chemistry and Chemical Biology, McMaster University, Hamilton, Ontario, L8S 4M1, Canada

[c] Department of Chemistry, The University of Hong Kong, Pokfulam Road, Hong Kong, P. R. China

Corresponding Author

* E-mail: g.chass@qmul.ac.uk, d.ditommaso@qmul.ac.uk

Contents

1. Computational details

1.1. Molecular dynamics simulations

Forcefield. The general AMBER forcefield (GAFF) was used to describe the ion–water and ion–ion interactions together with the SPC/E water model.[1] The ion–water and ion–ion interactions were described by the Lennard-Jones (LJ) GAFF potential [2] together with the SPC/E water model.[1] The structure, dynamics and kinetics properties of the hydrated magnesium ion (Mg^{2+}) computed with this potential are in good agreement with respect to quantum-chemical results and experimental data.[3] Moreover, using this forcefield allows the process of Mg-dehydration in the presence of other electrolytes to be simulated using a consistent set of LJ parameters. To derive the forcefield parameters within the framework of the GAFF, the optimised structures and molecular electrostatic potential of the molecular ions were computed at the HF/6-31G* level of theory with the Gaussian09 code.[4] Then, the Antechamber package was used to compute the atomic partial charges according to the restrained electrostatic potential formalism.[5] For the simulations of hydrated Ca^{2+}, we used the Buckingham potentials parameterized by de Leeuw [6] and Kerisit and Parker [7] together with SPC/E because the assessment of the Ca–O Buckingham potential parameterized by de Leeuw and Parker together with SPC/E was in excellent agreement with respect to DFT distances and energies.[8]

Simulation details. Classical MD simulations were performed using version GROMACS version 2016.3.[9,10] The leapfrog algorithm with a time step of 2 fs was used to integrate the equations of motion. Simulations were conducted in the isothermal (constant NVT) and isothermal-isobaric (constant NPT) ensemble at the target temperature T = 300 K and pressure P = 1 bar. The velocity rescale thermostat and the isotropic Parrinello-Rahman barostat were used with 0.4 ps and 2.0 ps as the thermostat and barostat relaxation times, respectively. The electrostatic forces were calculated by means of the particle-mesh Edwald approach with a cutoff of 1.2 nm. A 1.2 nm cutoff was also used for the van der Waals forces. The LINCS algorithm was used at each step to preserve the bond lengths. Periodic boundary conditions were applied throughout.

Metadynamics simulations. Free energy calculations were conducted computed by means of the well-tempered metadynamics-biased MD (MetaD) method,[11] using GROMACS 2016.3 equipped with the PLUMED 2.4.1 plugin.[12] The Mg−counterion distance were used as collective variable to compute the formation of ion pairs. Two collective variables were used to study the Mg^{2+} dehydration process: Mg−water distance; Mg-water coordination number (CN). The latter was defined using the continuous differentiable function:

$$CN = \sum_i \frac{1 - \left(\frac{r_i - d_0}{r_0}\right)^n}{1 - \left(\frac{r_i - d_0}{r_0}\right)^m} \qquad (1)$$

where r_0 = 1.1 Å, d_0 = 1.9 Å, n = 4, m = 8, r_i is the distance between the magnesium and the oxygen of *i*-th water molecule.[13] The free energy profiles were constructed by running metadynamics simulations with Gaussians laid every 1 ps and with an initial height equal to k_BT. The Gaussian widths were 0.2 and 0.1 along the distance and coordination number (CN), respectively.

Simulation protocol. The following protocol was used to generate electrolyte solutions and investigate the dynamics of water around Mg^{2+} in the presence of counterions X (F^-, Cl^-, NO_3^-,

HCO_3^-, CO_3^{2-}, SO_4^{2-}, HS^- and CH_3COO^-). We first conducted MD (NPT) simulation of around 1400 water molecules for 1 ns to generate an equilibrated aqueous solution. This was used to generate Mg^{2+} / X solutions by randomly replacing two water molecules with one magnesium ion and one (SO_4^{2-} and CO_3^{2-}) or two (F^-, Cl^-, HS^-, NO_3^-, HCO_3^-) counterions. We then conducted a series of NVT simulations for Mg–X separation distances (*d*) varying from approximately 13 Å to 4.5 Å using a harmonic bias potential with a force constant of 500 kJ.mol^{-1}. Starting from the last configuration corresponding to a Mg–X distance of approximately 4.5 Å, we have conducted MetaD (NVT) simulations using CN(Mg-H_2O) as collective variable for 100 ns. Test simulations were conducted for 1 μs to verify the full convergence of the free energy profiles computed using trajectories of 100 ns (see Fig. S1 below). Moreover, our previous assessment study of interatomic potential models for hydrated Mg^{2+} showed that a simulation period of 30 ns is enough to obtain convergent free energy profiles as a function of the Mg^{2+}-water coordination number (Fig. S1).[3] Similarly, we have conducted MetaD (NVT) simulations using CN(Mg-H_2O) as collective with Mg^{2+} and X forming a contact ion pair. In these MetaD simulations, the separation between Mg^{2+} and the counterion was kept at around 4.5 Å, which corresponds to a solvent shared $Mg^{2+}\cdots H_2O\cdots X$ ion pair, using a harmonic bias potential. We verified that throughout the simulations, the counterions did not enter the first coordination shell of Mg^{2+}.

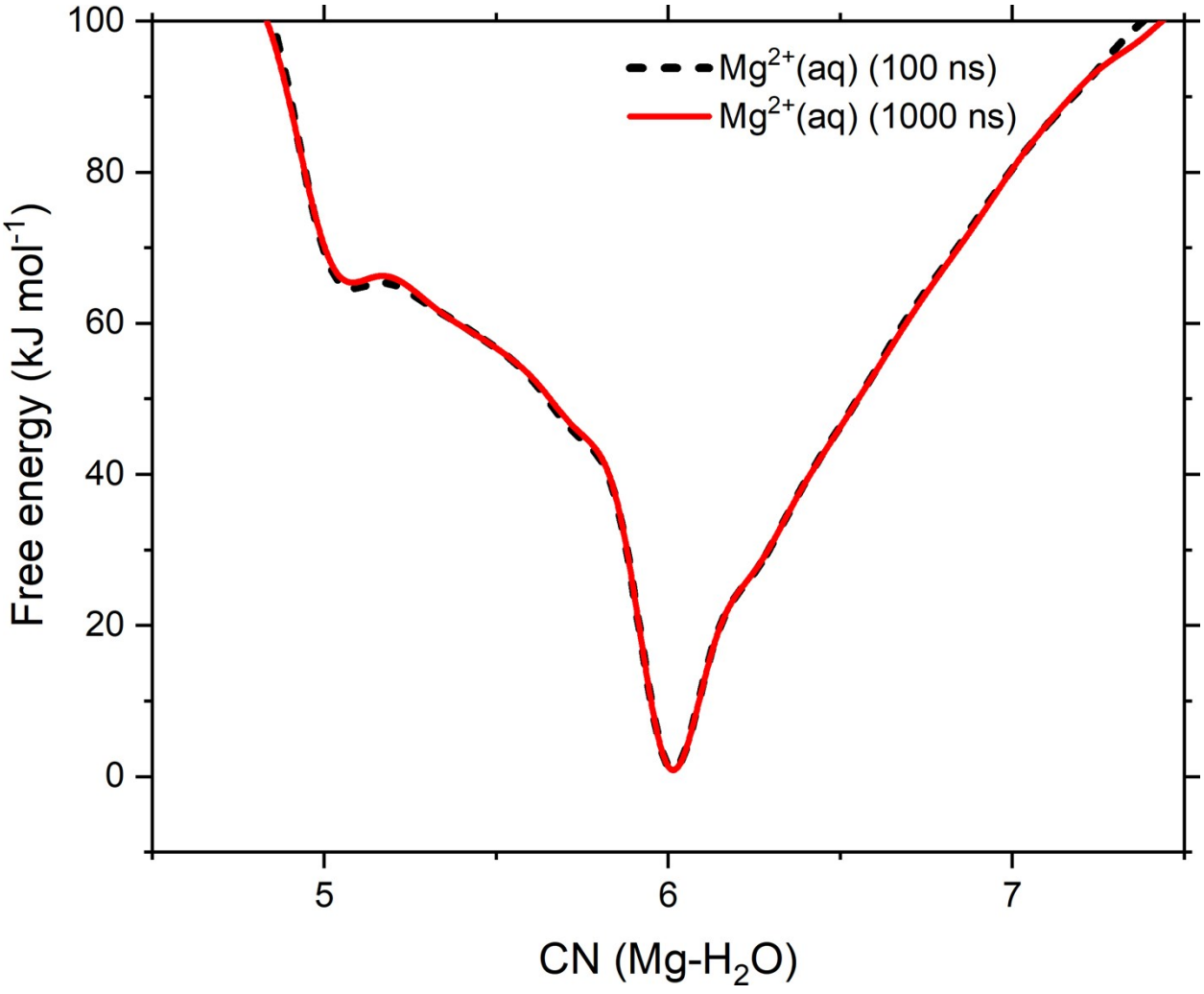

Figure S1. Comparison of the free energy profiles of hydrated Mg^{2+} as a function of the Mg^{2+}–H_2O water coordination number computed from 100 ns and 1000 ns MetaD simulations.

1.2. Details of simulated aqueous Mg^{2+} / X systems

TABLE S1. Details of the simulated electrolyte solutions: number of ions and H_2O molecules; cell length after the equilibration stage of classical MD in the NPT (1 atm, 300 K) ensemble.

System		n_{Mg}	n_X	n_{water}	Cell length (nm)
Mg^{2+}	1	1	0	883	3.000
Ca^{2+}	1	1	0	883	3.000
MgF_2 (aq)	1	1	2	1374	3.439
$MgCl_2$ (aq)	2	1	2	1345	3.446
$Mg(HCO_3^-)_2$ (aq)	3	1	2	1423	3.554
$Mg(CH_3COO^-)_2$ (aq)	4	1	2	1421	3.533
$Mg(HS^-)_2$ (aq)	5	1	2	1374	3.443
$MgCO_3$ (aq)	6	1	1	1442	3.544
$Mg(NO_3)_2$ (aq)	7	1	1	1374	3.456
$MgSO_4$ (aq)	8	1	1	1343	3.454

1.3. Electronic structure calculations

Complementary density functional theory calculations (DFT) were conducted with the Gaussian09 (G09) electronic structure code [4] using the Becke, 3-parameter, Lee–Yang–Parr (B3LYP) method,[15] together with the standard triple-zeta polarized 6-311G++(d,p) 6d basis sets. We conducted static geometry optimization of the hydrated magnesium clusters $Mg(H_2O)_5^{2+}$ and $Mg(H_2O)_6^{2+}$, of the hydrated solvent-shared ion pairs $[Mg(H_2O)_5]\cdot X^+$ and $[Mg(H_2O)_6]\cdot X^+$, and of the hydrated contact ion pairs $[MgX(H_2O)_4]\cdot H_2O^+$ and $[MgX(H_2O)_5]\cdot H_2O^+$ (X = Cl^-, F^-, HS^-). Solvent effects of water (ε= 78.4 at 298.15 K) were also taken into account by using the self-consistent reaction field polarizable continuum model (PCM).[16,17] All free energies reported were calculated from standard determinations emerging from the G09 output. The electronic properties of the optimised structures were analyzed by Bader's Atoms-In-Molecules (AIM) wavefunction analyses[18,19] to quantitatively characterize the topological properties of electron density distributions. Analyses were carried out on wavefunctions generated using the B3LYP/6-311G++(d,p)/PCM method on the geometry-optimized structures. All molecular graphs of wavefunctions reported in this paper have been constructed with the AIM2000 program package.[20]

2. Comparison of Mg^{2+} and Ca^{2+} dehydration

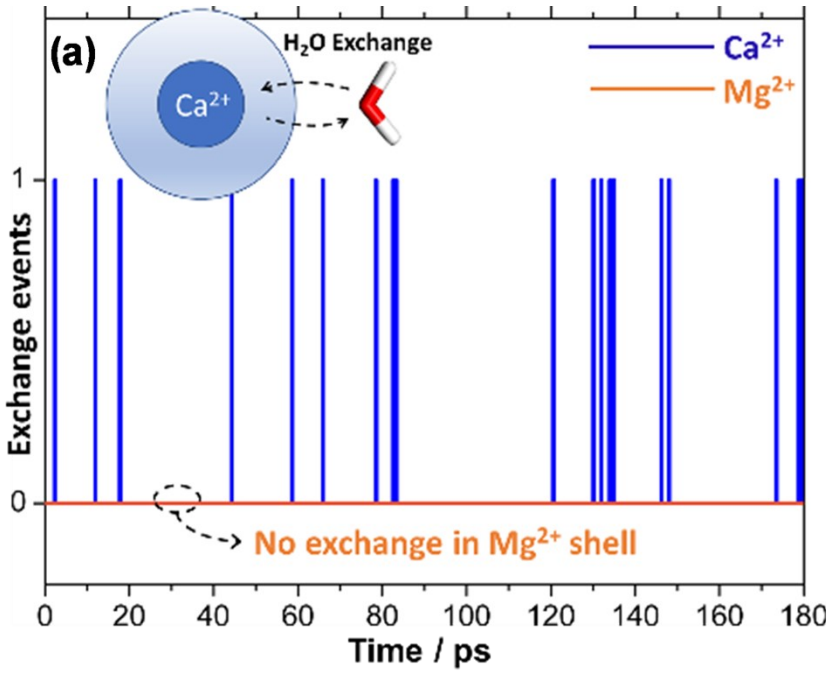

Figure S2. Water exchange in the first hydration shell of Mg^{2+} and Ca^{2+} during classical MD simulations. Water exchanges around in the first hydration shell of the cation determined using the "direct method".[21] Molecular dynamics trajectories were analysed for H_2O movements and whenever a molecule crossed the boundary of the cation coordination shell, its new position was path was followed; if its new position outside or inside this shell lasted for more than 0.5 ps, the event was counted as a real H_2O exchange. The first shell was defined to fall within the first minimum of the cation versus water oxygen radial distribution function.

3. Key structural parameters on the free energy as a function of the Mg^{2+} and additive distance

Table S2. Positions and free energies for the formation of contact ion pair (CIP) and solvent-shared ion pairs (SSHIP) between Mg^{2+} and the additive (X). Positions of CIP (r^{min}_{1}) and SSHIP (r^{min}_{2}) and of the maximum (r^{max}) on the free energy as a function of Mg^{2+}– X distance. Values are compared with the positions of first and second minima, and of the maximum (r^{max}) on the free energy profile for the removal of a single water molecule from the first hydration of Mg^{2+}. The values of the Gibbs free energy of reaction (ΔG) and standard Gibbs energy of activation (Δ‡G) are with respect to the free energy of the SSHIP. Distances in nm and free energies in $kJ.mol^{-1}$.

X	r^{min}_{1}	r^{max}	r^{min}_{2}	ΔG	Δ‡G
F^-	0.180	0.241	0.420	-41	58
Cl^-	–	–	0.478	–	–
HS^-	0.217	0.292	0.423	-18	56
HCO_3^-	0.181	0.250	0.391	-2	59
CH_3COO^-	0.197	0.255	0.380	1	41
NO_3^-	–	–	0.505	–	–
CO_3^{2-}	0.230	0.250	0.352	-26	29
SO_4^{2-}	0.190	0.260	0.406	-30	44
H_2O	0.200	0.280	0.420	-6.9	48

4. Free energy as a function of the Mg-H_2O coordination number

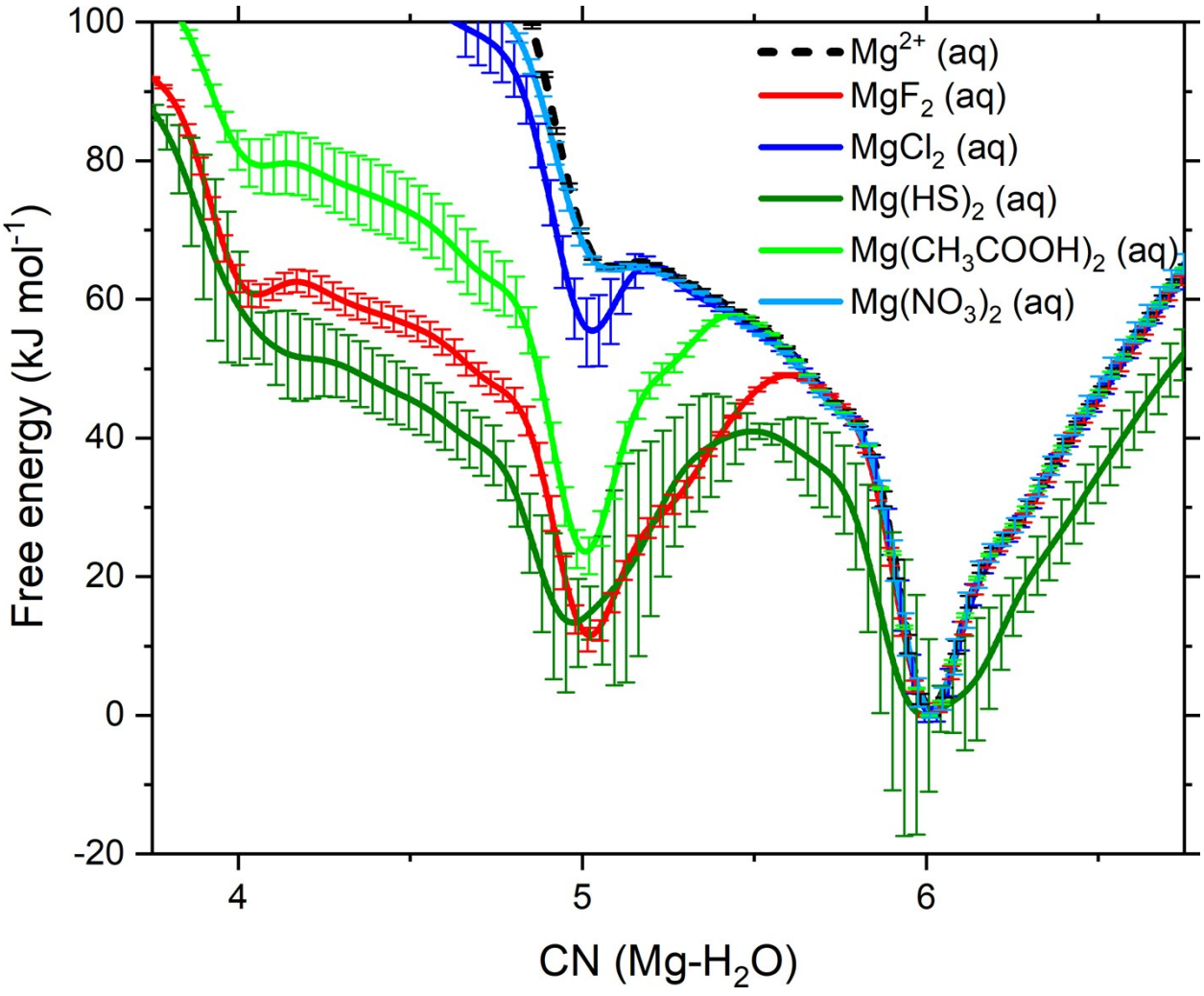

Figure S3. Free energy as a function of the Mg^{2+}-H_2O coordination number, CN(Mg-H_2O), for hydrated Mg^{2+} (single Mg^{2+}, no counterions) and solvated Mg^{2+} with a counterion in the second hydration shell. Standard deviation computed from the average of the profiles of four independent MetaD simulations (300 K).

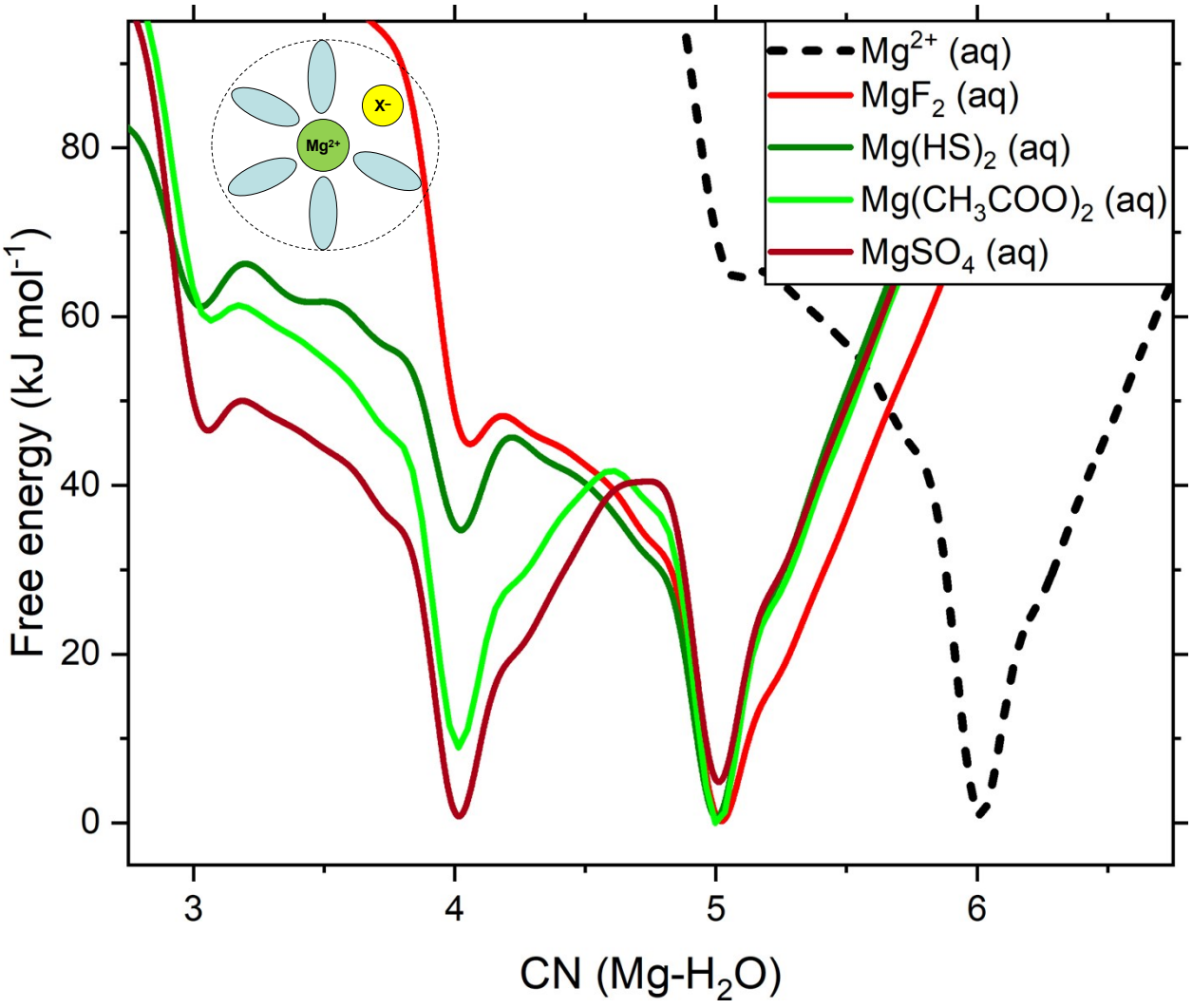

Figure S4. Free energy as a function of the magnesium-water coordination number, CN(Mg-H_2O), for a hydrated metal ion (single Mg^{2+}, no counterions) and of Mg^{2+} with a counterion in the first hydration shell.

5. Density functional theory calculations of hydrated Mg^{2+} clusters

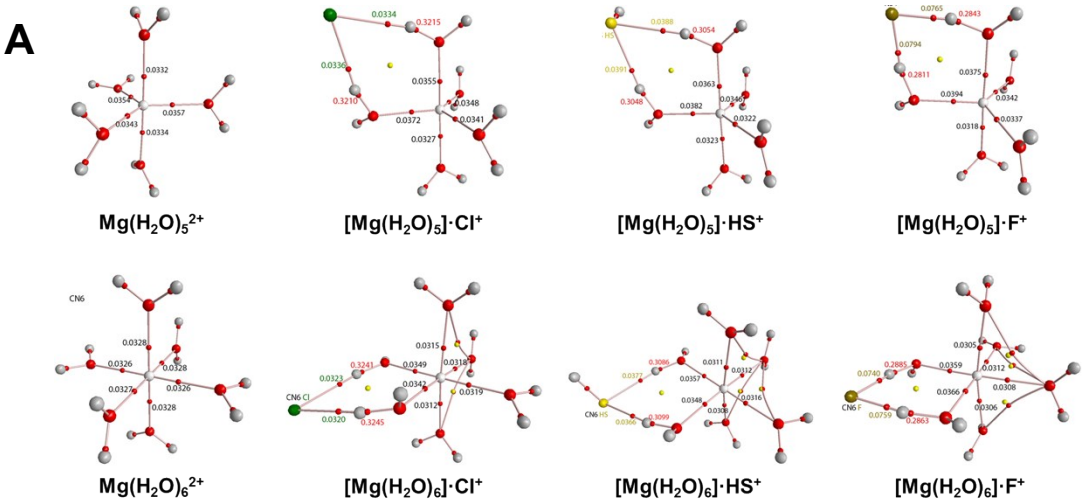

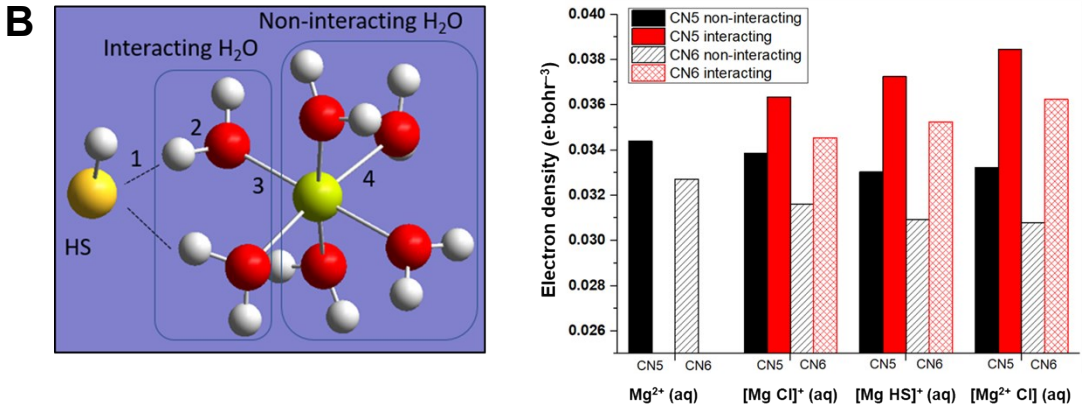

C

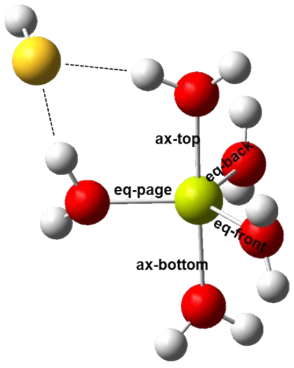

5-coordinate	0-5	Cl-5	HS-5	F-5	
eq-page	0.0357	0.0372	0.0382	0.0394	strengthening
ax-top	0.0332	0.0355	0.0363	0.0375	strengthening
eq-back	0.0343	0.0348	0.0346	0.0342	
eq-front	0.0354	0.0341	0.0322	0.0337	weakening
ax-bot	0.0334	0.0327	0.0323	0.0318	weakening
Average	0.0344	0.0349	0.0347	0.0353	
STDEV	0.0011	0.0017	0.0026	0.0031	
%dev (avg.)	100.0	101.3	102.7	102.7	

Figure S5. (A) Rho-b (ρ_b / ē·bohr^{-3}) values at the bond critical points obtained from Bader's AIM analyses of the wavefunction generated from the B3LYP/6-311++G(d,p) (SCRF=PCM, water) optimized structures of $Mg(H_2O)_n^{2+}$ and $[Mg(H_2O)_n]\cdot X^+$ (n = 5, 6). **(B)** Average ρ_b values between Mg and O for the interacting and non-interacting H_2O molecules in five-Mg and Mg-six-coordinated states. **(C)** Ongoing from $Mg(H_2O)_5^{2+}$, through $[Mg(H_2O)_5]\cdot Cl^+$, $[Mg(H_2O)_5]\cdot HS^+$, and

$[Mg(H_2O)_5]\cdot F^+$, the values of ρ_b for the water molecules in the “eq-page” and “ax-top” positions increase, corresponding to a strengthening of the Mg-H_2O bond interacting with the approaching X ion. However, the other three molecules weaken (values of ρ_b decrease), thus promoting further de-hydration. This is known as an allosteric effect, a classical trans-(axial)-directed via the axial-top strengthening at the expense of the axial-bottom ligand, which signals the 'kicking' of the axial-bottom ligating H_2O off the complex (dehydration), promoting change in coordination to four-coordinate.

Acknowledgements

This project (FUNMIN) is funded through the ACT programme (Accelerating CCS Technologies, Horizon2020 Project No 294766). Financial contributions made from Department for Business, Energy & Industrial Strategy (BEIS) together with extra funding from NERC and EPSRC research councils, United Kingdom, ADEME (FR), MINECO-AEI (ES)

References

1. H. J. C. Berendsen, J. R. Grigera and T. P. Straatsma, The missing term in effective pair potentials, *J. Phys. Chem.*, 1987, **91**, 6269–6271.

2. J. Wang, W. Wang, P. A. Kollman and D. A. Case, Automatic atom type and bond type perception in molecular mechanical calculations, *J. Mol. Graph. Model.*, 2006, **25**, 247–260.

3. X. Zhang, P. Alvarez-Lloret, G. Chass and D. Di Tommaso, Interatomic potentials of Mg ions in aqueous solutions: structure and dehydration kinetics, *Eur. J. Mineral.*, 2019, **31**, 275–287.

4. M. J. Frisch and D. J. Trucks, G. W.; Schlegel, H. B.; Scuseria, G. E.; Robb, M. A.; Cheeseman, J. R.; Scalmani, G.; Barone, V.; Mennucci, B.; Petersson, G. A.; Nakatsuji, H.; Caricato, M.; Li, X.; Hratchian, H. P.; Izmaylov, A. F.; Bloino, J.; Zheng, G.; Sonnenberg, J. L.; Had, in Gaussian, Inc Wallingford CT, 2009.

5. C. C. I. Bayly, P. Cieplak, W. D. Cornell and P. a Kollman, A well-behaved electrostatic potential based method using charge restraints for deriving atomic charges: the RESP model, *J. Phys. Chem.*, 1993, **97**, 10269–10280.

6. N. H. de Leeuw, Molecular dynamics simulations of the growth inhibiting effect of Fe^{2+}, Mg^{2+}, Cd^{2+}, and Sr^{2+} on calcite crystal growth, *J. Phys. Chem. B*, 2002, **106**, 5241–5249.

7. S. Kerisit and S. C. Parker, Free energy of adsorption of water and calcium on the [10 1 4] calcite surface., *Chem. Commun.*, 2004, 52–53.

8. D. Di Tommaso, E. Ruiz-Agudo, N. H. de Leeuw, A. Putnis and C. V. Putnis, Modelling the effects of salt solutions on the hydration of calcium ions, *Phys. Chem. Chem. Phys.*, 2014, 16, 7772–7785.

9. D. Van Der Spoel, E. Lindahl, B. Hess, G. Groenhof, A. E. Mark and H. J. C. Berendsen, GROMACS: Fast, flexible, and free, *J. Comput. Chem.*, 2005, **26**, 1701–1718.

10. B. Hess, C. Kutzner, D. Van Der Spoel and E. Lindahl, GRGMACS 4: Algorithms for highly efficient, load-balanced, and scalable molecular simulation, *J. Chem. Theory Comput.*, 2008, **4**, 435–447.

11. A. Barducci, G. Bussi and M. Parrinello, Well-Tempered Metadynamics: A Smoothly Converging and Tunable Free-Energy Method, *Phys. Rev. Lett.*, 2008, **100**, 20603.

12. G. A. Tribello, M. Bonomi, D. Branduardi, C. Camilloni and G. Bussi, PLUMED 2: New feathers for an old bird, *Comput. Phys. Commun.*, 2014, **185**, 604–613.

13. P. Raiteri and J. D. Gale, Thermodynamically Consistent Force Field for Molecular Dynamics Simulations of Alkaline-Earth Carbonates and Their Aqueous Speciation, *J. Phys. Chem. C*, 2015, **119**, 24447–24458.

14. F. J. Devlin, P. J. Stephens, J. R. Cheeseman and M. J. Frisch, Ab initio prediction of vibrational absorption and circular dichroism spectra of chiral natural products using density functional theory: α-Pinene, *J. Phys. Chem. A*, 1997, **101**, 9912–9924.

15. S. Miertuš, E. Scrocco and J. Tomasi, Electrostatic interaction of a solute with a continuum. A direct utilizaion of AB initio molecular potentials for the prevision of solvent effects, *Chem. Phys.*, 1981, **55**, 117–129.

16. G. Scalmani and M. J. Frisch, Continuous surface charge polarizable continuum models of solvation. I. General formalism, *J. Chem. Phys.*, 2010, **132**, 114110.

17. R. F. W. Bader, A quantum theory of molecular structure and its applications, *Chem. Rev.*, 1991, 91, 893–928.

18. R. F. W. Bader, Atoms in Molecules: A Quantum Theory, Oxford University Press, New York, 1995.

19. AIM2000 – A program to analyse and visualize atoms in molecules, *J. Comput. Chem.*, 2001, **22**, 545–559.

20. T. S. Hofer, H. T. Tran, C. F. Schwenk and B. M. Rode, Characterization of dynamics and reactivities of solvated ions by ab initio simulations., *J. Comput. Chem.*, 2004, **25**, 211–7.